

# The Role of Reaction Temperature and Cracking Catalyst Characteristics in Determining the Relative Rates of Protolytic Cracking, Chain Propagation, and Hydrogen Transfer

Avelino Corma,<sup>\*,1</sup> Pablo J. Miguel,<sup>†</sup> and Antonio V. Orchillés<sup>†</sup>

<sup>\*</sup>Instituto de Tecnología Química, UPV-CSIC, Universidad Politécnica de Valencia, Camino de Vera s/n, 46071 Valencia, Spain; and  
<sup>†</sup>Departament d'Enginyeria Química, Universitat de València, Dr. Moliner 50, 46100 Burjassot, Valencia, Spain

Received February 8, 1993; revised June 2, 1993

The cracking of isobutane on USY zeolites with different unit cell size has been studied in the temperature range 400–500°C, using an experimental apparatus which makes it possible to follow the reaction at very short times on stream. By measuring product initial selectivities it has been found that protolytic cracking and bimolecular reactions take place on Brønsted acid sites. In this way the contributions of bimolecular and monomolecular processes have been established. Bimolecular reactions involving hydride transfer have been separated from those responsible for chain transfer and those producing hydrogen transfer. Chain transfer accounts for the chain propagation in paraffin cracking, while hydrogen transfer produces the extra paraffin amounts obtained in these reactions. Hydrogen transfer reactions increase, but chain transfer reactions decrease when the unit cell size increases. From energetic considerations, the influence of the zeolite catalyst and reaction conditions on the controlling step in isobutane cracking can be suggested. © 1994 Academic Press, Inc.

## INTRODUCTION

During the earlier development of commercial catalytic cracking there was controversy on the mechanism of paraffin cracking on acid catalysts (1–5). In the last 10 years a sensible effort has been made to clarify this matter (6–15). It has been established that the initiation of paraffin cracking may occur through the formation of a carbenium ion on a Brønsted acid site by protonation of a C–C bond followed by cracking to give a paraffin and an adsorbed carbenium ion (6–8). From this perspective the mechanism for paraffin cracking could be visualized through a chain mechanism including the initiation step as described above, chain propagation involving hydride transfer between an adsorbed carbenium ion and a reactant paraffinic molecule followed by  $\beta$ -scission (2, 5, 9), and termination, which would involve the desorption

of the surface carbenium ions formed in previous steps as an olefin (6).

Several studies have been carried out to clarify the contribution of each of the three steps to the observed rate during paraffin cracking (5, 8–12). In this way, it has been shown (6) that high temperatures and smaller zeolite pores favor initiation via protolytic cracking and termination, versus chain propagation via hydride transfer. Others (8), working with *n*-alkanes, have concluded that on zeolite Y, protolytic cracking is favored over  $\beta$ -scission when the framework Si–Al ratio is increased. Moreover, the rate for the disappearance of the reactant via protolytic and  $\beta$ -scission type cracking has also been calculated (10, 11).

Recently, Hall *et al.* (13, 14) have shown the utility of isobutane as a cracking test molecule. Indeed, in a molecule like this, protolytic attack can occur relatively easily on a C–C bond, since after cracking a secondary carbenium ion is left on the surface. In addition, proton attack can also occur on the C–H bond of the tertiary hydrogen, since in this case H<sub>2</sub> is formed while a stable tertiary carbenium ion is left on the catalyst surface.

In this work we have used this molecule as reactant, and cracking has been carried out on zeolite Y with different unit cell sizes at different reaction temperatures. The reaction has been carried out using an experimental set which makes it possible to follow the reaction at very short times on stream (TOS). This methodology makes it possible not only to avoid problems when comparing catalysts with different activity/deactivation rates and under different reaction conditions, but also to follow the evolution of product distribution from the very first moments of the reaction. In this way, it is shown that, besides the bimolecular hydride transfer reaction which is responsible for the chain transfer, other bimolecular reactions also occur. Thus, in this work, we try to differentiate between the bimolecular hydride transfer which corresponds to chain propagation and which does not modify

<sup>1</sup> To whom correspondence should be addressed.

the theoretical 1:1 paraffin to olefin ratio that can be expected in the products, and the bimolecular hydrogen transfer which is responsible for olefin saturation and formation of aromatics and coke (5, 16).

## EXPERIMENTAL

### Materials

Two samples of USY zeolite, with unit cell sizes 24.46 and 24.25 Å, were prepared in the following way: a NaY (Si/Al = 2.4 sample was twice  $\text{NH}_4^+$  exchanged at 80°C, and in this way 70% of the original  $\text{Na}^+$  was removed. The  $\text{NaNH}_4\text{Y}$  zeolite was steam-calcined (100% steam) at 550°C, and after this was again  $\text{NH}_4^+$  exchanged and calcined at 500°C for 2 h. The resultant sample was named as USY-1. Sample USY-2 was obtained by steam calcination of USY-1 at 700°C, followed by  $\text{NH}_4^+$  exchange, and a new steam-calcination at 750°C. The characteristics of the samples are given in Table 1.

### Procedure

Catalytic experiments at atmospheric pressure were carried out in a continuous fixed bed, microcatalytic, glass reactor at 400, 450, and 500°C. A  $\text{N}_2/\text{isobutane}$  reactant mixture in a 9 to 1 molar ratio and with a total flow of  $7.617 \times 10^{-5} \text{ mol} \cdot \text{s}^{-1}$  was fed into the reactor. The flows were measured and controlled by *caudalimeters* (Brooks). The exit of the reactor was connected to a computer controlled heated multiloop sampling valve (0.25 ml loop volume). A hydrocarbon gas detector was placed right at the exit of the external loop of the valve in order to precisely determine the time for the first molecule of hydrocarbon to arrive into the multiloop valve. This was defined as zero time and the first loop was filled up. After this, the next loops were automatically filled at TOS of 6, 18, 39, 90, 180, 600, and 1800 s. After this, the gases in the loops were automatically injected into the G.C., separated in a Supelco Petrocol 100 m capillary column, and analyzed using two detectors, thermal conductivity and flame ionization, in series.

TABLE 1

Characteristics of the Catalysts Used in This Work

	USY-1	USY-2
U.c.s. (Å)	24.46	24.25
Cryst. (%Y)	107	77
$\text{Na}_2\text{O}$ (wt%)	0.24	0.22
Al/u.c. <sup>a</sup>	25.5	0.9
Surface area ( $\text{m}^2/\text{g}$ )	838	540
Framework Si/Al	5.2	172

<sup>a</sup> Calculated from Fichtner-Schmittler equation (17).

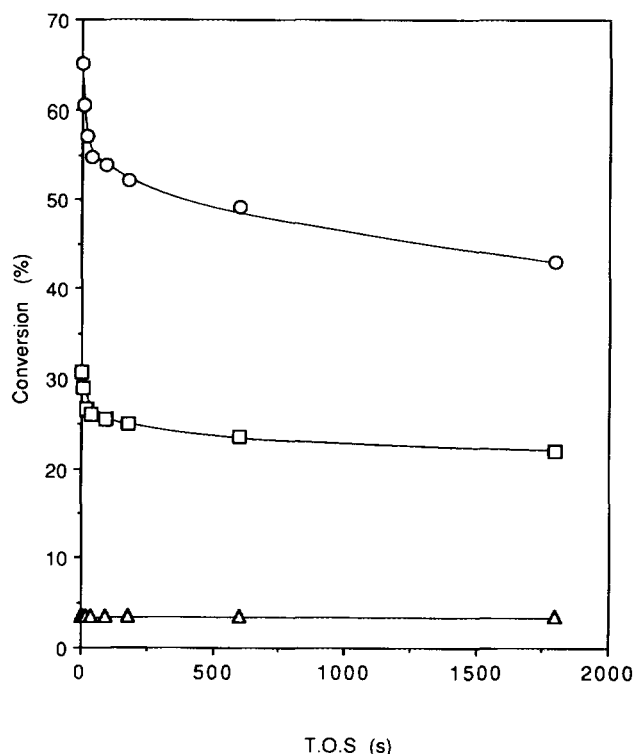


FIG. 1. Influence of time on stream on instantaneous conversion in isobutane cracking at 500°C.

This procedure was followed working at different space velocities ( $F/W$ ), from  $5.85 \times 10^{-6}$  to  $8.19 \times 10^{-5} \text{ mol reactant} \cdot \text{s}^{-1} \cdot \text{g catalyst}^{-1}$ , obtained by changing the amount of catalyst between 0.1001 and 1.4 g.

The rate of methane and hydrogen formation and the total rate of reactant disappearance were calculated by the following equations:

$$\text{rate of product} = \text{Yield of product (\%)} \times F/W \times 1/100$$

$$\text{total rate} = \text{Conversion (\%)} \times F/W \times 1/100.$$

## RESULTS AND DISCUSSION

When the instantaneous conversion was varied between 0 and 65%, on zeolite USY-1, it was observed (Fig. 1) that catalyst deactivation does not occur at low conversion. Changes in conversion and selectivity with time on stream were observed at conversion levels higher than 15% (Figs. 1 and 2). It has to be remarked that under our experimental conditions most of the deactivation has occurred in the first 20 s; thus all the experimental work reported in the literature, which has been performed in a conventional way, taking samples at times on stream longer than 20 s, was not able to detect this catalyst deactivation. It should also be taken into account that when the

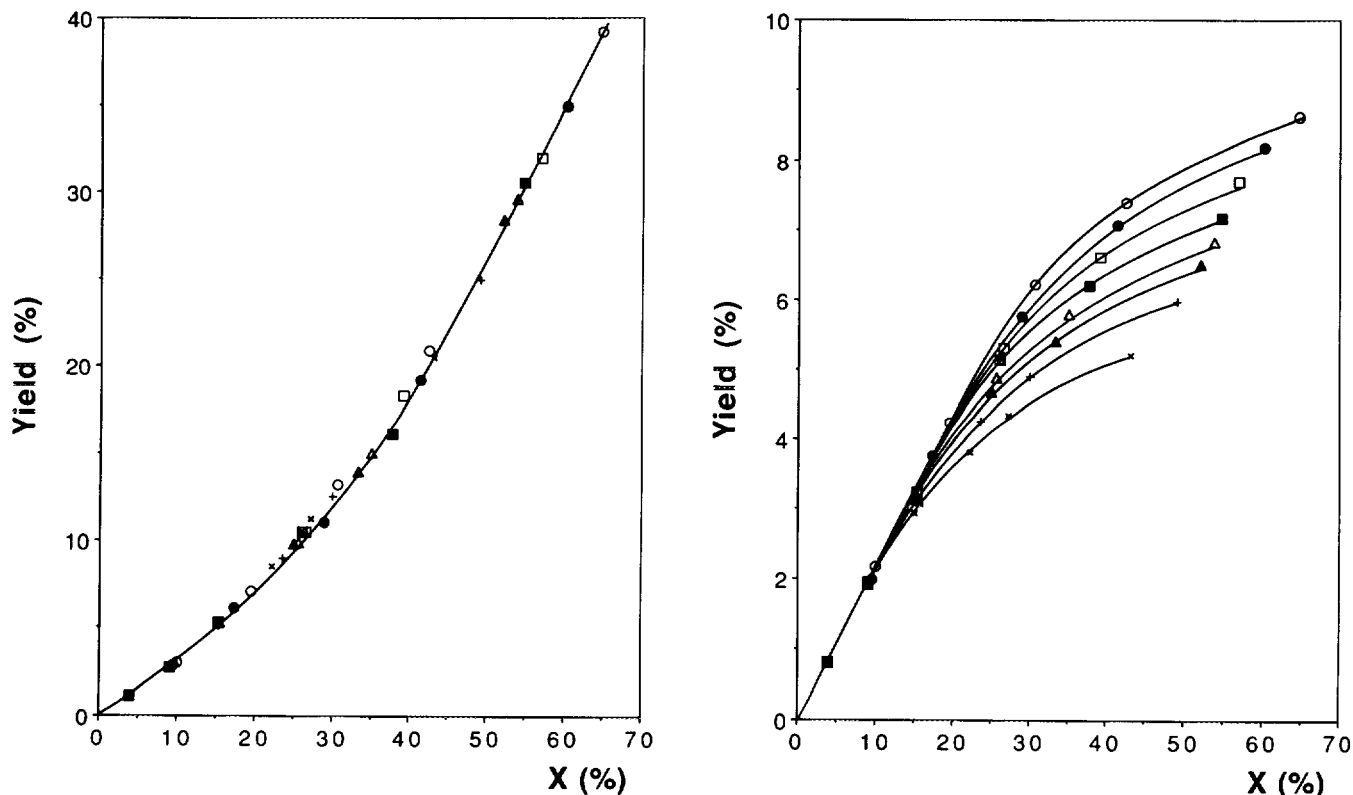


FIG. 2. Yields of propane (a) and propylene (b) in isobutane cracking on USY-1 zeolite at 500°C. TOS (s): (○) 0, (●) 6, (□) 18, (■) 39, (△) 90, (▲) 180, (⊕) 600, (▲) 1800.

purpose of cracking studies is to contribute to understand the behavior of, and to better design, real cracking catalysts, it becomes crucial to know what occurs at very short times on stream. Then, by using the experimental set described here, it has been possible to see that on zeolite USY-2, and when working at 400°C and low conversions (<5%), the yields to methane and H<sub>2</sub> were slightly higher in samples taken at the shortest times on stream (0–6 seconds) than in those obtained at longer times.

Figure 2 shows as an example of the type of curves obtained the yield vs conversion for propane and propylene. From this figure it can be seen that initial selectivities for those products identify as primary can be obtained from the ratio yield/conversion at conversion levels <5%. Following this methodology the initial selectivities of primary products have been calculated and are given in Table 2. The most important primary products detected were hydrogen, methane, propane, propylene, butenes, and *n*-butane. At higher conversion levels, ethane, branched C<sub>6</sub>, and dibranched species were also detected, and they are considered as secondary products. Consequently, and in agreement with previous work (14), it can be said that isobutane suffers isomerization, cracking, and dehydroge-

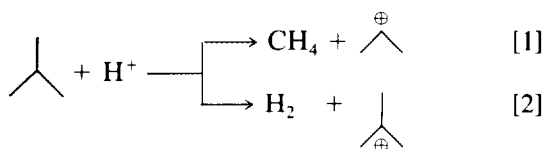
TABLE 2  
Initial Molar Selectivities (%) Obtained from the Yield/Conversion Ratio for the Primary Products in Isobutane Cracking

	USY-1			USY-2		
	400°C	450°C	500°C	400°C	450°C	500°C
Convers. (%)	3.10	4.75	3.91	0.369	0.728	2.22
Hydrogen	30.0	31.5	35.5	5.12	13.1	39.4
Methane	6.19	12.7	24.7	3.10	7.59	19.5
Ethylene	—	1.25	1.73	—	—	—
Propylene	3.77	9.48	21.8	2.15	7.49	21.3
Propane	33.63	31.4	30.1	104.8	87.7	32.5
Isobutylene	5.50	7.34	13.0	3.15	8.22	19.5
<i>n</i> -Butenes	5.07	8.41	15.1	1.97	7.55	24.5
<i>n</i> -Butane	38.9	29.75	16.0	3.16	3.18	8.46
Isopentane	7.63	8.07	2.71	—	—	1.28
Isopentenes	—	0.209	0.172	—	—	—
<i>n</i> -Pentane	0.266	0.410	0.138	—	—	—
<i>n</i> -Pentenes	—	—	—	—	—	—
Coke <sup>a</sup>	10.1	8.41	5.62	9.83	7.06	0.635

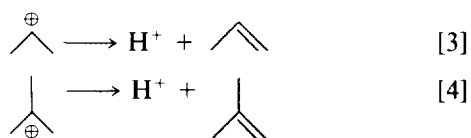
<sup>a</sup> Initial weight selectivity (%).

nation reactions, and Brønsted acids are the active sites responsible for the initiation.

Indeed the protonation of the C–C and C–H bonds gives the pentacoordinate carbonium ions which, when cracked, give methane and H<sub>2</sub>, leaving on the surface the corresponding carbenium ions:



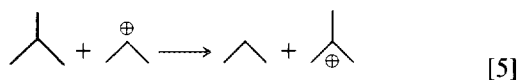
The desorption of these carbenium ions gives propylene and isobutene, and their amounts depend on the average life time of the adsorbed carbenium ions:



The results from Table 2 show accordingly that the selectivity to propylene and isobutene decreases when the reaction temperature decreases and the acid strength of the Brønsted acid sites increases.

However, when initial selectivities are quantitatively analyzed it can be seen (Table 2) that the material balance from reactions [1–4] is not closed. Indeed, propane appears as a primary reaction product and *n*-butane is a major product. Besides, the molar ratios for H<sub>2</sub>/C<sub>4</sub> and C<sub>1</sub>/C<sub>3</sub> are lower than 1. These results indicate that other reactions besides those described in reactions [1] and [3], and which were the ones considered in a previous work (12), are also important even when working at low levels of conversion.

As a first approximation it could be accepted that some of the propane can come from disproportionation of two reactant molecules to give propane and C<sub>5</sub>, since C<sub>5</sub> species are also observed in the products. Nevertheless, the contribution of this reaction must be limited, since the C<sub>3</sub>/C<sub>5</sub> ratio is much higher than 1. Propane can also be formed by hydride transfer during the bimolecular chain propagation reaction, from a reactant molecule and the propyl carbenium ion left on the surface after the protolytic cracking of isobutane:



Propane can also be formed by bimolecular hydrogen transfer from coke precursors to C<sub>3</sub><sup>+</sup> or to readsorbed propylene.

The formation of *n*-butane, could be explained through a unimolecular isomerization of the *tert*-butyl carbenium ion followed by chain hydride transfer on the *sec*-butyl carbenium formed (12). This is not a easy process (18) since it involves the formation of primary carbenium ions along the process. An additional route for the isomerization of isobutane, which would be in agreement with the product distribution given in Table 2, would go through a bimolecular process as has been postulated for *n*-butane isomerization (19–21). This would involve the formation of carbenium ions of more than four carbon atoms, which by cracking can form *n*-butane, as well as C<sub>5</sub> products, which are also observed. This process is called alkylation followed by cracking. Thus, we conclude that, even at conversion levels as low as 3% and very short times on stream, the olefins formed as primary products have already gone secondary bimolecular reactions.

From all this one can consider that during the reaction of isobutane on USY zeolites two groups of reactions are occurring. The first group involves unimolecular reactions such as the protonation of the C–C and C–H bonds, followed by protolytic cracking to give methane and hydrogen, respectively. The second group accounts for the bimolecular reactions occurring between the adsorbed carbenium ions formed in reactions [1] and [2] and other molecules of the reaction mixture to carry out the chain propagation through hydride transfer, alkylations followed by β-scission, and hydrogen transfer leading to olefin saturation and coke. A proposed set reactions occurring during isobutane cracking on zeolite can be seen in Table 3. There it is observed that isomerization to *n*-butane and disproportionation to C<sub>5</sub> and C<sub>3</sub> species take place via alkylation followed by β-scission reactions. Thus *n*-butane could be obtained, for instance, through the following consecutive reactions: dimerization between isobutene and a *tert*-butyl ion, skeletal isomerization, β-scission of 2,2,3-trimethyl pentyl ion, *n*-butene adsorption, and hydride transfer from *i*-butane. In contrast, C<sub>5</sub> species could be obtained by dimerization between isobutene and a *tert*-butyl ion followed by β-scission. On the other hand, coke is a product for which the mechanism and structure are not well established. In this sense, reaction 29 in Table 3 must be interpreted as a hydrogen transfer reaction in which by means of a hydride and a proton transfer from an adsorbed carbenium ion molecule, the saturation of olefins occurs, while aromatics and coke are produced.

Then the monomolecular mechanism generates the carbonium ions that after cracking produces the carbenium ions which in turn are responsible for a mechanism of chain propagation via the hydride transfer reactions (reaction [5]), which produces the *tert*-butyl carbenium ion. The desorption of the carbenium ion constitutes the chain termination and regenerates the Brønsted site which could

TABLE 3  
Reaction Network for Isobutane Cracking on Zeolites

Reaction	Type
$H^+ + \text{isobutane} \longrightarrow H_2 + \text{isobutyl}^+$	Protolytic [1]
$H^+ + \text{isobutane} \longrightarrow CH_4 + \text{isobutyl}^+$	Protolytic [2]
$\text{isobutyl}^+ \rightleftharpoons \text{isobutene} + H^+$	Desorption-Adsorption [3]
$\text{isobutyl}^+ \rightleftharpoons \text{isobutene} + H^+$	Desorption-Adsorption [4]
$\text{isobutyl}^+ \rightleftharpoons \text{isobutene} + H^+$	Desorption-Adsorption [5]
$\text{isobutyl}^+ \rightleftharpoons \text{isobutene} + H^+$	Desorption-Adsorption [6]
$\text{isobutyl}^+ \rightleftharpoons \text{isobutene} + H^+$	Desorption-Adsorption [7]
$\text{isobutyl}^+ \rightleftharpoons nC_5^+ + H^+$	Desorption-Adsorption [8]
$\text{isobutyl}^+ \rightleftharpoons \text{isobutyl}^+$	Charge Isomerization [9]
$\text{isobutene} + \text{isobutyl}^+ \rightleftharpoons \text{isobutyl}^+$	Alkylation [10]
$\text{isobutene} + \text{isobutyl}^+ \rightleftharpoons \text{isobutyl}^+$	Alkylation [11]
$\text{isobutyl}^+ \rightleftharpoons \text{isobutyl}^+$	Skeletal Isomerization [12]
$\text{isobutyl}^+ \rightleftharpoons \text{isobutyl}^+$	Skeletal Isomerization [13]
$\text{isobutyl}^+ \rightleftharpoons \text{isobutyl}^+$	Skeletal Isomerization [14]
$\text{isobutyl}^+ \rightleftharpoons \text{isobutyl}^+$	Skeletal Isomerization [15]

TABLE 3—Continued

Reaction		Type
		Skeletal Isomerization [16]
		Skeletal Isomerization [17]
		Skeletal Isomerization [18]
		Charge Isomerization [19]
		$\beta$ -Scission [20]
		$\beta$ -Scission [21]
		$\beta$ -Scission [22]
		$\beta$ -Scission [23]
		$\beta$ -Scission [24]
		Chain Propagation [25]
		Chain Propagation [26]
		Chain Propagation [27]
		Chain Propagation [28]
		Hydrogen Transfer [29] Coke

start a new reaction chain. It appears clear that in systems with relatively long propagation chains, the initiation reactions should be more important in the very first moments, when the "carbenia surface" (22) is being formed. This

has been observed in our case when using zeolite USY-2 as catalysts since then the selectivity to methane and  $H_2$  is higher in the very first moments of the reaction than at longer times on stream.

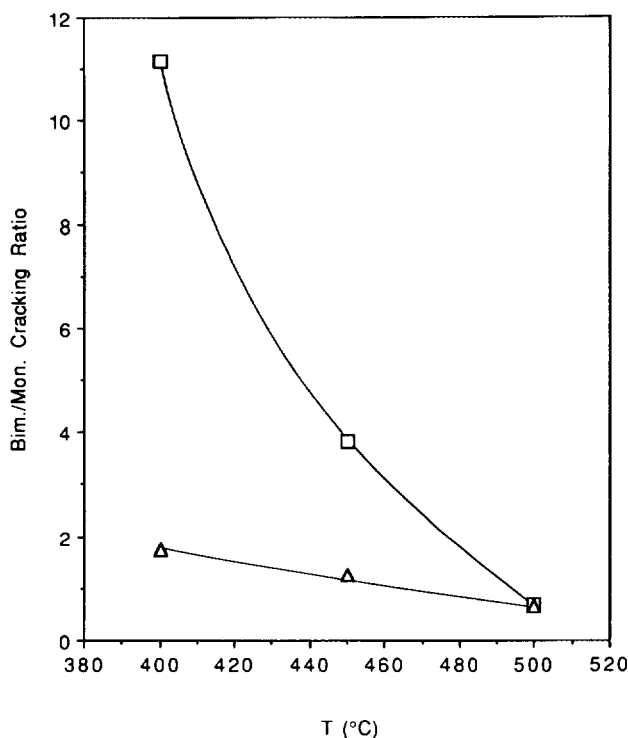


FIG. 3. Bi- and monomolecular cracking ratios for USY-1 ( $\Delta$ ) and USY-2 ( $\square$ ) catalysts, calculated from initial selectivities.

#### *Influence of Catalyst and Process Conditions on Reaction Mechanism*

It should be possible to calculate in our case the contribution of the monomolecular mechanism from the initial selectivities of methane plus  $H_2$  (Y). Therefore, according to Table 2, the contribution of the bimolecular processes responsible for the chain propagation is given by  $100 - [(CH_4) + (H_2)]$  initial selectivities. The ratio between the bi- and monomolecular processes  $(100 - Y)/Y$  has been plotted in Fig. 3, and the number of isobutane molecules which intervene in the chain propagation process per initiation event is indicated. This parameter is also known as chain length (12) and cracking mechanism ratio (11). In Fig. 3 it can be seen that the bimolecular processes associated with chain propagation increase with decreasing reaction temperature and increasing framework Si/Al ratio of the zeolite, this being especially notorious at lower reaction temperatures. Indeed at higher temperatures the influence of the framework Si/Al ratio is lower.

The evolution of  $(100 - Y)/Y$  with the unit cell size of zeolite is surprising, considering that when unbranched paraffins are cracked the bimolecular reactions are disfavored when the unit cell size decreases, or in general when the Si/Al ratio increases. There is a difference, however, in our case, which may explain this apparent paradox. This is that when branched paraffins are used

as feed, tertiary carbenium ions are formed when a hydride ion is transferred from the reactant to the surface carbenium ion. On the other hand, when a hydride ion is transferred from an *n*-paraffin, a less stable secondary carbenium ion is formed. Therefore, branched paraffins are more prompt to perform hydride transfer than *n*-paraffins and consequently a higher ratio of bi- to monomolecular reactions will be found. Moreover, in the case of unbranched paraffins, the initiation via protolytic cracking involves the formation, as intermediate, of quite unstable primary carbenium ions which can be stabilized on the very strong acid sites generated at relatively high Si/Al ratios. In this case the stronger acid sites are determinative for the monomolecular process. In the case of branched paraffins less strong acid sites are necessary for initiation. However, there is no doubt that the average lifetime of the adsorbed carbenium ions is longer on stronger acid sites, and therefore the probabilities for bimolecular reactions to occur will strongly increase.

However, in a recent work (12), it was reported that the chain propagation decreases when the framework Si/Al ratio increases. Moreover, in that work the  $H_2/CH_4$  molar ratio found was always below 1, while in our case it is always above 1. These differences could be explained taking into account that in the previous work the amount of  $H_2$  formed was underestimated (23), and so was the  $H_2/CH_4$  ratio. This error in the determination of  $H_2$  could affect the values determined for the initiation and chain propagation.

At this point it is convenient to separate the bimolecular reactions responsible for chain propagation, in which hydride transfer from the reactant to adsorbed carbenium ions is determinative, from the bimolecular hydrogen transfer from an adsorbed molecule leading to coke, which does not involve one molecule of reactant. On USY-2 and at 400°C reaction temperature, most of the isobutane reacts through bimolecular processes (Fig. 2). In this case the monomolecular processes mainly act to generate the "carbenia surface," and therefore to generate the active sites for the propagation chain. On the other hand, it is possible to calculate the probabilities of alkylation between isobutene and carbenium ions involved in isomerization and disproportionation by grouping reactions in Table 3 and using selectivities given in Table 2. Following this methodology the calculated values are 0.63, 0.44, and 0.44 for USY-1 and 0.57, 0.55, and 0.51 for USY-2 at 400, 450, and 500°C, respectively. This behavior of the bimolecular chain propagation and alkylation-cracking reactions with respect to unit cell size indicates that the density of acid sites is not the only controlling parameter.

Concerning coke formation, results from Fig. 4 show that the average lifetime of the carbenium ions is not the only factor which controls the formation of coke; other factors related to the density of framework Al, and there-

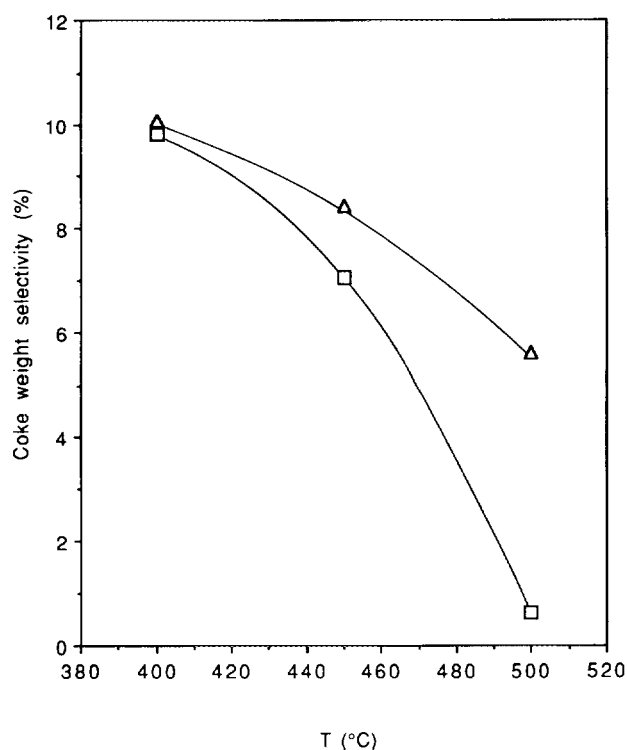


FIG. 4. Coke weight selectivities for USY-1 ( $\Delta$ ) and USY-2 ( $\square$ ) catalysts.

fore to adsorption properties, play an important role. The amount of coke decreases with increasing zeolite framework Si/Al ratio, indicating that the hydrogen transfer reactions involved in coke formation do evolve with unit cell size in a different manner than chain propagation and alkylation-cracking. This difference suggests that bimolecular hydrogen transfer is a concerted mechanism involving two adjacent sites, or a site and an adjacent adsorbed molecule, while the other bimolecular reactions only involve one active site.

#### Energetics of the Different Processes Involved in *i*-Butane Cracking

From the yields of methane and  $H_2$  obtained at a constant reactant partial pressure and contact times given in Table 4, the rates of formation of  $CH_4$  and  $H_2$  were calculated. From values obtained at different reaction temperatures (Fig. 5), the apparent activation energies were calculated. In the case of USY-2 zeolite catalyst similar activation energies,  $39.6 \pm 5.3$  and  $37.5 \pm 4.5$  kcal  $\cdot$  mol $^{-1}$ , were obtained for  $H_2$  and  $CH_4$  formation, respectively. This behavior is the same as that observed by Krannila *et al.* (24) for *n*-butane cracking on an HZSM-5 zeolite. This can be explained by assuming that in the highly dealuminated USY-2 zeolite, as in HZSM-5, the controlling step in the protolytic cracking of the isobutane

TABLE 4

Methane and Hydrogen Yield (%) at Constant Partial Pressure of Reactant (10.132 kPa), and Space Velocity in Isobutane Cracking

	USY-1			USY-2		
	400°C	450°C	500°C	400°C	450°C	500°C
Hydrogen	0.930	1.495	1.389	0.0189	0.0953	0.874
Methane	0.192	0.604	0.967	0.0115	0.0553	0.432
F/W $\times 10^6$ (mol/s $\cdot$ g)	8.18	20.5	82.1	6.76	6.76	6.87

is the formation of the pentacoordinated carbonium ion but not the C-C or C-H cracking. However, on high Al content USY-1 zeolite, the activation energies for  $CH_4$  and  $H_2$  formation were  $40.6 \pm 0.4$  and  $28.0 \pm 0.6$  kcal  $\cdot$  mol $^{-1}$ , respectively.

However, we have to consider that  $H_2$  can also be produced by dehydrogenation during "coking" on zeolites. Thus, in a high Al content USY-1 zeolite (unit cell size 24.46 Å), the total amount of coke, as well as the level of dehydrogenation, is higher than in a highly dealuminated USY-2 zeolite (unit cell size 24.25 Å). Thus, especially on USY-1,  $H_2$  can also be produced by coke

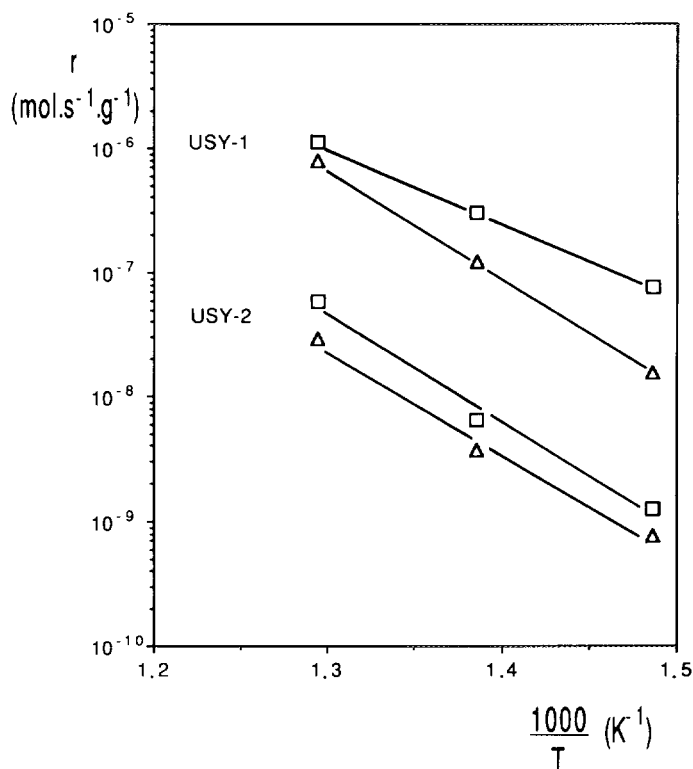


FIG. 5. Arrhenius plot of methane ( $\Delta$ ) and hydrogen ( $\square$ ) production (isobutane partial pressure = 10.132 kPa).



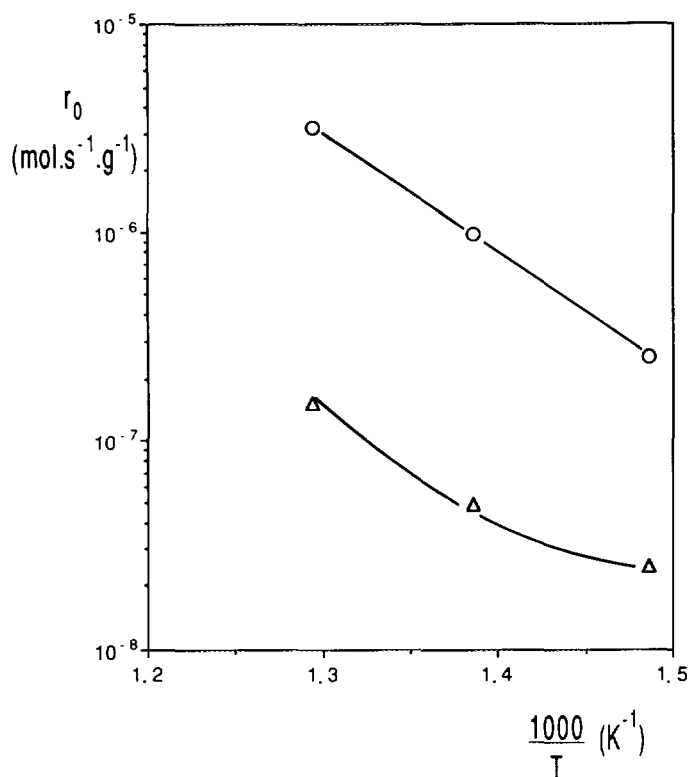


FIG. 6. Reaction rate ( $\text{mol} \cdot \text{g}^{-1} \cdot \text{s}^{-1}$ ) at reactant partial pressure of 10.132 kPa in isobutane cracking on USY-1 (○) and USY-2 (△) vs temperature.

dehydrogenation and therefore the activation energy calculated from the yields of  $\text{H}_2$  does not represent only the net C–H breaking in isobutane. To check this possibility the coke formed on the surface of the USY-1 at 500°C and 1800 s of TOS was studied by IR using self-supporting wafers. In this case a very intense band at  $1546 \text{ cm}^{-1}$  was observed, indicating the presence of a sensible amount of coke (the zeolite was completely black after reaction). However, in the  $2900\text{--}3100 \text{ cm}^{-1}$  region no bands were detected with could be associated to C–H bonds, indicating that the coke formed must be highly dehydrogenated. A simple  $\text{H}_2$  balance, taking coke dehydrogenation into account, does indicate that the activation energy for the purely isobutane dehydrogenation should be sensibly higher than the  $28 \text{ kcal} \cdot \text{mol}^{-1}$  obtained when considering the total  $\text{H}_2$  formed.

When the activation energy for the global disappearance of isobutane is calculated (Fig. 6), it can be seen that while the Arrhenius equation does apply reasonably well on USY-1, a bad fitting is observed on USY-2. In this catalyst the activation energy increases with increasing reaction temperature, i.e., when the ratio of bi- to monomolecular reactions decreases (see Fig. 3). Then, if in a first approximation two "activation energies" are calculated on USY-2 at 500 and 450°C, in which monomolecular

reactions are predominant, and at 450 and 400°C, in which bimolecular reactions become more important, 25.3 and  $13.1 \text{ kcal} \cdot \text{mol}^{-1}$  are obtained, respectively. These values suggest that the activation energies for the bimolecular processes are sensibly lower than those involved in unimolecular protolytic cracking. From this, one may conclude that in the global cracking process the controlling step may be either the protonation-cracking itself or the chain propagation, depending on the reaction temperature. In other words, at lower reaction temperatures, hydride transfer is the controlling step during paraffin cracking, while at higher temperatures, the C–C bond rupture or the formation of the pentacoordinated carbonium ion is the controlling step. This is more clearly visible when the low unit cell size zeolite is used as catalyst.

### CONCLUSIONS

A new experimental system has been developed which makes it possible to perform cracking measurements at very short times on stream. This allowed us to see during isobutane cracking on USY zeolites, that protolytic cracking to give  $\text{CH}_4$  and  $\text{H}_2$  occurs first on the catalysts. Then other bimolecular reactions, i.e., hydride transfer responsible for chain propagation, alkylation followed by  $\beta$ -scission, and hydrogen transfer, start to be important.

The ratio of bimolecular to monomolecular cracking decreases with increasing temperature and increasing unit cell size of Y zeolite. However, at 500°C, that ratio is the same for two USY samples with 24.46 and 24.25 Å unit cell size.

The decrease in the length of chain propagation with increasing temperature is much higher on the zeolite with lower unit cell size. This result is related to the average life time of the cations on the surface.

Moreover, chain hydride transfer evolves with reaction temperature in a different way than  $\text{H}_2$  transfer. Indeed, acid site density does not appear as the main controlling parameter, while this becomes the most important variable for hydrogen transfer, decreasing when the unit cell size decreases.

Finally, it has been shown that the controlling step in catalytic cracking may change with reaction temperature and zeolite catalyst. For instance, at lower cracking temperatures, the controlling step for cracking is the bimolecular chain hydride transfer. However, at higher temperatures, the controlling step is the protonation cracking.

### REFERENCES

1. Voge, H. H., "Catalysts" (P. H. Emmett, Ed.), Vol. VI. Reinhold, New York, 1958.
2. Greenselder, B. S., Voge, H. H., and Good, G. M., *Ind. Eng. Chem.* **41**, 2573 (1949).
3. Weisz, P. B., *Annu. Rev. Phys. Chem.* **21**, 175 (1970).

4. Tung, S. E., and McIninch, E., *J. Catal.* **10**, 166 (1968).
5. Gates, B. C., Katzer, J. R., and Schuit, G. C. A., "Chemistry of Catalytic Processes." McGraw-Hill, New York, 1979.
6. Haag, W. O., and Dessau, R. M., in "Proceedings, 8th International Congress on Catalysis, Berlin, 1984." Vol. 2, p. 11,305. Dechema, Frankfurt-am-Main, 1984.
7. Corma, A., Planelles, J., Sánchez-Marín, J., and Tomás, F., *J. Catal.* **93**, 30 (1985).
8. Gianetto, G., Sansare, S., and Guisnet, M., *J. Chem. Soc. Chem. Commun.*, 1302 (1986).
9. Withmore, F. C., *J. Am. Chem. Soc.* **54**, 3274 (1932).
10. Ono, Y., and Kanae, K., *J. Chem. Soc. Faraday Trans.* **87**, 663 (1991).
11. Wielers, A. F. H., Vaar Kamp, M., and Post, M. F. M., *J. Catal.* **127**, 51 (1991).
12. Shertukde, P. V., Marcelin, G., Sill, G. A., and Hall, W. K., *J. Catal.* **136**, 446 (1992).
13. Lombardo, E. A., Pierantozzi, R., and Hall, W. K., *J. Catal.* **110**, 171 (1988).
14. Lombardo, E. A., and Hall, W. K., *J. Catal.* **112**, 565 (1988).
15. Riekert, L., and Zhou, J., *J. Catal.* **137**, 437 (1992).
16. Pine, L. A., Maher, P. J., and Wachter, W. A., *J. Catal.* **85**, 466 (1984).
17. Fichtner-Schmittler, H., Lohse, V., Engelhart, G., and Patzelova, V., *Cryst. Res. Technol.* **19**, K1 (1984).
18. Stocker, M., Hemmersbach, P., Roeder, J. H., and Grepstad, J. K., *Appl. Catal.* **25**, 223 (1986).
19. Bearez, C., Chevalier, F., and Guisnet, M., *React. Kinet. Catal. Lett.* **22**, 405 (1983).
20. Krupina, N. N., Proskurmin, A. L., and Dorogochinskii, A. Z., *React. Kinet. Catal. Lett.* **32**, 135 (1986).
21. Fajula, F., *Stud. Surf. Sci. Catal.* **20**, 361 (1985).
22. Corma, A., Planelles, J., Sánchez-Marín, J., and Tomás, F., *J. Catal.* **93**, 30 (1985).
23. Petunchi, J. O., Sill, G. A., and Hall, W. K., *J. Catal.*, in press.
24. Krannila, H., Haag, W. O., and Gates, B. C., *J. Catal.* **135**, 115 (1992).